ORIGINAL PAPER

Stimulation of human olfactory receptor 17-40 with odorants probed by surface plasmon resonance

Irina Benilova · Vladimir I. Chegel · Yuri V. Ushenin · Jasmina Vidic · Alexey P. Soldatkin · Claude Martelet · Edith Pajot · Nicole Jaffrezic-Renault

Abstract We report here the results of human olfactory receptor (OR) 17-40 stimulation with some odorants probed by means of the double-channel surface plasmon resonance platform NanoSPR-6. OR 17-40 tagged with N-terminal cmyc sequence was heterologously co-expressed with $G\alpha_{olf}$ protein in yeast, and receptor-carrying nanosomes were prepared from yeast membrane fraction. Then, receptors were specifically captured via anti-cmyc antibody attached to the gold-coated substrate in orientated or random way. Measurement of odorants effects were carried out in the presence of GTP-γ-S in differential mode in order to compensate bulk changes of refractive index. For the first time, biosensing efficiency of olfactory films was discussed in terms of their thickness and $G\alpha_{olf}$ accessibility to GTP-γ-S. Bell-shaped response profile with two maxima (near 1 nM and near 1 μM) was established for helional, which is documented as highly specific agonist of OR 17-40. Unrelated odorant heptanal used as control, did not evoke significant variations of differential signal.

Keywords Biofilm · Thickness · Nanosome · Olfactory receptor · Surface plasmon resonance

Abbreviations

GPCRs	G protein-coupled receptors
ORs	Olfactory receptors
SAM	Self-assembled monolayer
SPR	Surface plasmon resonance
PBS	Phosphate-buffered saline
AFM	Atomic force microscopy
CV	Cyclic voltammetry

I. Benilova (✉) · C. Martelet
Laboratoire Ampère, Ecole Centrale de Lyon,
36 Avenue Guy de Collongue, 69134 Ecully Cedex, France
e-mail: i_skry@yahoo.com

V. I. Chegel · Y. V. Ushenin
Lashkaryov Institute of Semiconductor Physics NASU,
45 Avenue Nauki, 03028 Kyiv, Ukraine

J. Vidic · E. Pajot
Neurobiologie de l'Olfaction et de la Prise Alimentaire,
Récepteurs et Communication Chimique, INRA,
Domaine de Vilvert, 78352 Jouy-en-Josas Cedex, France

I. Benilova · A. P. Soldatkin
Laboratory of Biomolecular Electronics,
Institute of Molecular Biology and Genetics NASU,
150 Zabolotnogo Street, 03143 Kyiv, Ukraine

N. Jaffrezic-Renault
Laboratoire des Sciences Analytiques, UMR-CNRS 5180,
Université Claude Bernard, Lyon 1,
43 Boulevard du 11 Novembre 1918,
69622 Villeurbanne Cedex, France

Introduction

Recent advances in the pharmacology of olfactory receptors (ORs) and other G protein-coupled receptors (GPCRs) result mainly from the development of in vitro screening of receptors agonists (Tollin et al. 2003; Minic et al. 2005a; Li et al. 2006; Milligan 2006). There is a growing interest in elaboration of biosensors based on the ORs expressed homologously (Liu et al. 2006) and heterologously (Araneda et al. 2004; Ko and Park 2005; Sung et al. 2006; Vidic et al. 2006; Hou et al. 2007; Marrakchi et al. 2007), employed in the membrane fraction or in the whole cell coupled to a solid transducer. Biosensor platforms for ligand profiling and GPCRs deorphanization can be based on the direct monitoring either of agonist binding to receptor or of spatial

molecular events triggered by agonist-stimulated receptor at the biointerface (Li et al. 2006).

The pharmacological data available on mammalian ORs include various dose-response profiles. A typical adsorption curve with a remarkably broad linear part (10^{-11}–10^{-3} M) was obtained by means of the quartz crystal microbalance technique for heterologously expressed rat OR I7 exposed to its agonist octanal (Ko and Park 2005). The increase in calcium signal of OR I7 from isolated olfactory neurons was sigmoid within the concentration range 10^{-7}–10^{-5} M of octanal (Araneda et al. 2004). Other data obtained from intracellular calcium and bioluminescence assays revealed the response pattern of heterologously expressed OR I7 and OR 17-40 to be bell-shaped within the concentration range 10^{-14}–10^{-3} M of their agonists octanal and helional, respectively (Araneda et al. 2000; Levasseur et al. 2003; Minic et al. 2005a; Ko and Park 2006).

The goal of this work was to investigate a pattern of G protein-coupled OR 17-40 response to its specific odorant helional. Two different OR 17-40-carrying biofilms were designed and their biosensing efficiency was studied by using an original surface plasmon resonance (SPR) sensor platform NanoSPR-6. Topography of olfactory biofilms was probed by means of atomic force microscopy (AFM) and cyclic voltammetry (CV), and its impact on the biosensing properties of films was discussed.

Experimental

Biomaterials

Human OR 17-40 tagged with cmyc sequence on the N-terminus and $G\alpha_{olf}$ protein were co-expressed in yeast *Saccharomyces cerevisiae* (strain MC18, Crowe et al. 2000) and membrane fraction was prepared as previously described (Minic et al. 2005a; Vidic et al. 2006). Stock suspension of membrane fragments with protein content 3 mg ml^{-1} was aliquoted and stored at $-80°$C. Anti-cmyc monoclonal antibody (Ab) was obtained from Roche Molecular Biochemical and biotinylated by means of DSB-X™ Biotin Protein Labeling Kit (Molecular Probes, Leiden, Netherlands). Stock solution of biotinylated Ab (2.55 mg ml^{-1}) was divided into aliquots and stored at $-20°$C.

GTP-γ-S (93% purity), bovine serum albumin (BSA; 98% purity) were purchased from Sigma, neutravidin—from Pierce.

Chemicals

16-Mercaptohexadecanoic acid (MHDA; 90% purity) and 1,2-dipalmitoyl-*sn*-glycero-3-phosphoethanolamine-N-biotinyl sodium salt (biotinyl-PEA) were purchased from

Aldrich and Avanti Polar Lipids, respectively. Potassium ferricyanide (3-/4-) was obtained from Sigma, Ethanol (99.8%), HCl (37%), HNO_3 (65%), H_2O_2 (30%) and NH_4OH (25%)—from Fluka.

Dimethyl sulfoxide (DMSO) and heptanal were obtained from Sigma. Helional was a kind gift from Givaudan-Roure (Switzerland).

As a working buffer, a phosphate-buffered saline (PBS) was used with the following composition: 8 mM Na_2HPO_4, 1.5 mM KH_2PO_4, 3 mM KCl, 150 mM NaCl, pH 7.0. All reagents for preparation of PBS were of analytical grade. Ultrapure water with resistivity 18.2 MΩ cm was used for the PBS preparation.

Sensor chips and SPR spectrometer

A novel Kretschmann-type SPR spectrometer NanoSPR-6 (model 421, NanoSPR, USA) with two optical channels and light-emitting diode light source ($\lambda = 650$ nm) was used in this work. A high refraction index of the prism ($n = 1.61$) and a broad dynamic range (up to 19° in air) of the SPR instrument enabled a high quality of the computer fitting of the experimental data with a theoretical curve. The SPR data were processed by means of the NanoSPR-6 software (version 6.0). The SPR sensorgrams represented real-time changes in the minimal reflectivity angle and could be recorded both in custom and differential mode (delta between working and reference channels) using double channel teflon flow cell.

Glass supports (TF-1 glass, 20 mm × 20 mm) coated with a thin chromium sublayer (5 nm) and a polycrystalline gold layer (50 nm) were provided by NanoSPR.

Pretreatment of gold surface

Before experiments, each gold-coated substrate was cleaned by a mixture "aqua regia": H_2O + HCl + HNO_3, 16 + 3 + 1, v/v, during 1.5 min, then with a basic mixture (H_2O + H_2O_2 + NH_4OH, 5 + 1 + 1, v/v) during 30 s and finally, thoroughly rinsed with water.

Biofilm design

Two different biofilm architectures were studied: Au + (MHDA + biotinyl-PEA) + neutravidin + biotinylated Ab + OR 17-40 ("A1" biofilm), and Au + biotinylated Ab + OR 17-40 ("A2" biofilm).

To obtain self-organized heterogeneous layer onto gold, 1 mM MHDA and 0.1 mM biotinyl-PEA were dissolved in ethanol and incubated with freshly cleaned chip for 21 h at room temperature. MHDA was fixed onto Au via chemisorption, whereas biotinyl-PEA was inserted between long-chain thiols via hydrophobic interactions.

Such self-assembled monolayer (SAM) provides a good basis for the further anchoring of biomolecules to the surface. To elute unfixed molecules, the chip was rinsed with ethanol, and dried under nitrogen flow.

Neutravidin (0.5 μM) and/or biotinylated Ab (0.5 μM) were subsequently run through both channels from the stock solution (0.3 ml in PBS) at the flow rate 0.02 ml min^{-1}. Before formation of any upper molecular layer the previous one was rinsed with PBS during 5–15 min.

In order to saturate all non-specific adsorption sites on modified surface, Ab layer was blocked by BSA (0.5 mg ml^{-1} in PBS), which was run on a chip at the flow rate 0.02 ml min^{-1}.

Preparation and immobilization of OR 17-40

Stock suspension of OR 17-40 in membrane fraction was diluted in PBS on ice down to the protein concentration 70 μg ml^{-1} and 0.3 ml of this suspension was treated in the ultrasonic bath Bandelin Sonorex Super RK 102H (35 kHz, 140 W) in ice-cold water for 20 min in order to obtain an homogeneous suspension of membrane vesicles called nanosomes due to their size (Vidic et al. 2006). Afterwards, the suspension was immediately run on the chip at the flow rate 0.02 ml min^{-1}. One nanosome of 50 nm diameter could bear up to ten ORs (Vidic et al. 2007). Orientation of ORs in lipid bilayer seems to vary. Most probably, ORs may be orientated in both directions: N-terminus located outside or inside the vesicles, sonication apparently supporting an orientation of membrane proteins opposite to that in the cell (Monk et al. 1989; Seckler and Wright 1984).

Preparation of odorants

Stock 0.1 M solutions of odorants were prepared freshly on the day of experiment in DMSO; further dilutions (from 10^{-4} to 10^{-12} M) were obtained by successive 1:10 dilutions in PBS. The blank probes at the various dilutions were prepared replacing the odorant by PBS. Blank solutions were run via the reference channel simultaneously with odorant probe to compensate possible bulk effect of DMSO in odorant detection. Additionally, each odorant and blank probe contained 10 μM of GTP-γ-S prepared on ice from the 1 mM solution.

Cyclic voltammetry

Surface plasmon resonance substrate modified with biofilm A1 or A2 was transferred into an electrochemical glass cell ($V = 5$ ml) and used as a working electrode. The measurements were conducted at room temperature by an impedance analyzer Voltalab 40 in 4 mM potassium ferricyanide in PBS. Saturated calomel electrode from Radiometer Analytical was employed as a reference, a platinum plate—as an auxiliary electrode. Scan rate was 50 mV s^{-1}.

AFM

The substrates were imaged with Nanoscope III microscope (Digital Instrument, USA). A pyramidal silicon tip RTESP (Veeco) with a spring constant of 20–80 Nm^{-1} was used. The cantilever oscillated at 300 kHz resonance frequency with free amplitude of 2 V. All experiments were performed in air at room temperature and relative humidity of 60%. Images were taken in tapping mode to avoid damaging the surface of the sample.

Results

Orientated and random immobilization of antibodies

Receptors carried by nanosomes were immobilized via interactions of cmyc sequence with anti-cmyc monoclonal Ab attached to the gold in orientated or random way. In the first case, Abs were uniformly attached to the neutravidin layer (Fig. 1a, b).

Random immobilization involved Abs' adsorption on the freshly cleaned gold (Fig. 2a, b).

A signal for specific anchoring of biotinylated Ab to the neutravidin was about two times lower than a response to its direct adsorption on gold probably due to the limited quantity of biotinyl-PEA affinity sites at the surface.

To estimate the thickness of each molecular layer, the experimental SPR spectra were fitted to the theoretical curves on the basis of five-phase Fresnel calculations using the Nelder–Mead algorithm of minimization (Beketov et al. 1998). As a basis, an effective refractive index of $n = 1.36$ was used for protein layers (Beketov et al. 1998) and of $n = 1.46$ for a membrane vesicle (Johnsen and Widder 1999). The shape of biomolecules and nanosomes was considered as globular. The calculated values of thickness are presented in Table 1.

The spatial orientation of immobilized Ab is crucial for OR capture since the latter is based on the highly specific interaction via cmyc tag. While the ratio Abs:nanosomes in case of biofilm A1 is close to 1, it is equal to 7 for the A2 suggesting that probably only ~11% of immobilized antibodies are properly orientated. Therefore, a random orientation of Ab layer resulted in a nanosome layer of comparatively low density (Table 1).

Electrical properties of biofilms

At it was revealed by CV measurements, SAM-based A1 architecture was a highly insulating film (Fig. 3). The
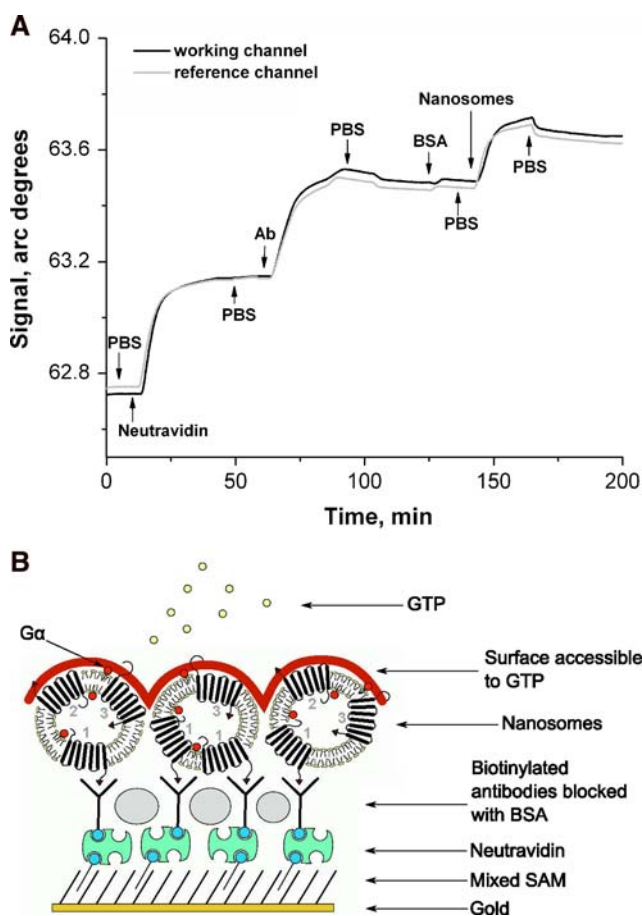
Fig. 1 **a** Sensorgram of layer-by-layer assembly of A1 biofilm. The SPR sensorgrams were recorded in differential mode relative to reference channel. **b** Scheme of multilayer A1. Possible orientations (1, 2, 3) of Gα_olf coupled receptors in a nanosome are described in Table 2

electron transfer through the A2 was 50% weaker in comparison with redox kinetics on bare Au (Fig. 3 inset).

The insulating properties of A2 increased after its overnight incubation in PBS at room temperature. In order to clarify this phenomenon, a biofilm consisting only of randomly adsorbed Ab was probed under the same conditions. This layer of antibodies demonstrated an increased penetrability to redox couple after 12 h of contact with PBS (data not shown). Therefore, an increase of insulating properties of A2 biofilm can be attributed to the nanosomes' fusion on the top of sensor surface. Since redox peaks did not completely disappear, one might conclude that the membrane vesicles did not merge into a continuous layer; therefore, the fusion of nanosomes on the electrode surface could be only partial, corroborating recently reported AFM-based data (Vidic et al. 2007).

Topography of biofilms

Atomic force microscopy images of biofilms were taken after the second day of odorant screening. Clear difference
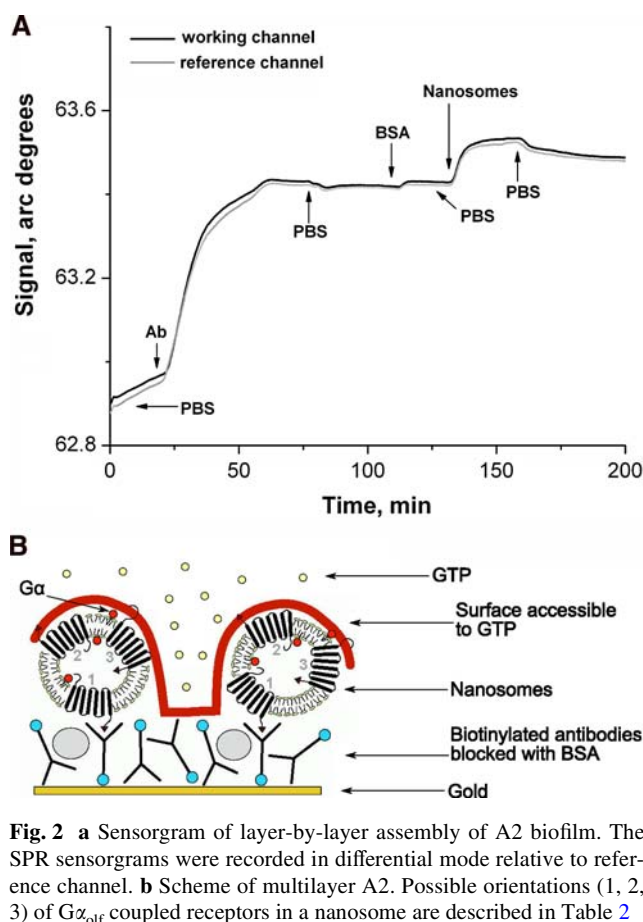

Fig. 2 **a** Sensorgram of layer-by-layer assembly of A2 biofilm. The SPR sensorgrams were recorded in differential mode relative to reference channel. **b** Scheme of multilayer A2. Possible orientations (1, 2, 3) of Gα_olf coupled receptors in a nanosome are described in Table 2

in relief porosity was observed between working "spots" of A1 (Fig. 4a) and A2 (Fig. 4b) structures. The surface profile of A1 biofilm was rather smooth due to the proper orientation of multilayer or to the collapsing of immobilized nanosomes, whether initial or after work with the surface. In the calculations of thickness (Table 1), the coefficient of coverage of A1 with membrane biomaterial was taken as 1. The A2 surface coverage was estimated as 0.25 from the level of porosity observed.

Detection of odorants

An olfactory signal is transmitted into sensory neurons via an interaction of OR with heterotrimeric G protein located on the cytoplasmic face of neuron ciliae membrane (Bourne 1997). Activated OR promotes the liberation of GTP-bound Gα subunit from Gβγ dimer (Jones and Reed 1989; Bourne 1997; Cao and Huang 2005; Birnbaumer 2007). Surface-grafted membrane fragments bearing Gα_olf and ORs present a complex biorecognition unit where the above-described conformational changes of receptor and Gα_olf are thought to occur upon OR stimulation with odorant. Possible orientations of Gα_olf-coupled OR in nanosome are shown in

Table 1 Surface plasmon resonance responses to the layer-by-layer formation of A1 and A2 biofilms and calculated thickness of each molecular layer

Layer	A1, arc degrees	A1, effective thickness, nm	A2, arc degrees	A2, effective thickness, nm
MHDA-based self-assembled monolayer	Not available	1.9 (Dannenberger et al. 1997)	–	–
Neutravidin	0.34 ± 0.03	15 ± 1	–	–
Biotinylated antibodies	0.26 ± 0.02	12.5 ± 0.75	0.42 ± 0.07	18.5 ± 1
BSA	0.01 ± 0.00	0.5 ± 0.1	0.02 ± 0.01	0.9 ± 0.2
OR 17-40-bearing nanosomes	0.20 ± 0.09	11 ± 0.75 ($V = 1$)	0.06 ± 0.01	11 ± 0.75 ($V = 0.25$)
Total thickness of multilayer on gold, nm	~ 41		~ 30	

V is a coefficient of surface coverage with lipidic biomaterial estimated from the AFM data shown in Fig. 4. The error values mentioned represent intersensor standard deviation, $n = 3$–4

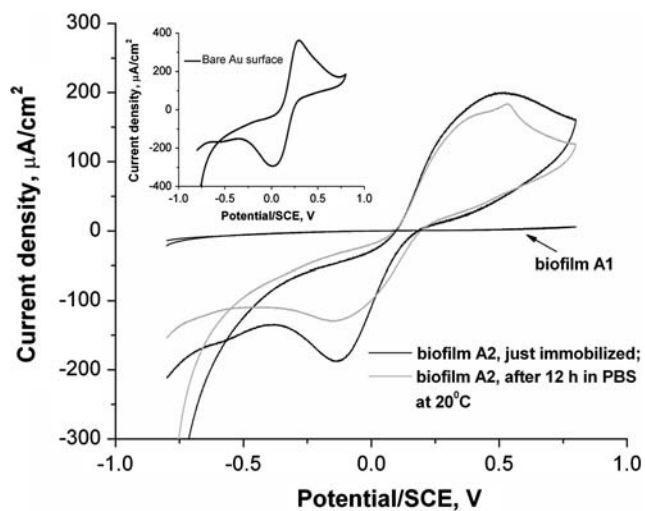*MHDA* 16-mercaptohexadecanoic acid, *BSA* bovine serum albumin

Fig. 3 Cyclic voltammograms of biofilms A1 and A2. Inset: cyclic voltammogram of bare gold substrate. Redox probe: 4 mM potassium ferricyanide in PBS; *SCE* saturated calomel electrode

Figs. 1b and 2b, and a potential biorecognition efficiency of each configuration is schematized in Table 2.

Two odorants, helional and heptanal, were tested on A1 and A2 in the concentration range from 10^{-12} to 10^{-5} M. Helional is documented as a cognate odorant for OR 17-40 (Wetzel et al. 1999; Levasseur et al. 2003). Measurements were carried out in the differential mode at the day of biofilm formation (1st day of work) and were continued the next day. Observed SPR signals had a dose-dependent "dissociation" character, (Fig. 5 inset). Olfactory sensitivity of thicker A1 biofilm with comparatively dense nanosomes layer was weaker than that of the A2 (Fig. 5); therefore, we did not apply a detailed range of helional concentrations to A1 in order to reveal its response profile.

Sensitivity of receptors to helional after the overnight storage of SPR substrate coated with biofilm A1 decreased

essentially, while A2 demonstrated only a slight relative decrease in response (Fig. 5).

During 2 days of work with the same A2 biofilm we observed the same pattern of response to helional (Fig. 6). Meanwhile, A2 sensitivity to the unrelated odorant heptanal remained insignificant somewhat increasing at 10^{-9} M after the overnight storage (Fig. 6).

Discussion

As it can be seen from Table 1, the biofilm A2 based on the randomly oriented Abs was at least 27% thinner than the A1 biofilm. Low thickness of A2 and its high porosity (Fig. 4b) resulted in better accessibility of $G\alpha_{olf}$ protein to GTP-γ-S could explain a surprisingly better sensitivity of A2 to helional. Presence of pores in A2 initially originates from the random orientation of Abs and relates to their inability to bind a large amount of nanosomes. From this point of view, the thickness of both A1 and A2 nanosome layer is similar, whereas the refractive index of the latter is smaller. The thickness of nanosome layer in both cases, close to twice a lipid bilayer thickness, demonstrates a flattening of the nanosomes down to partial collapsing.

The possible reasons of signal decrease after 12 h storage of SPR chip at room temperature are: (1) loss in receptor and/or $G\alpha_{olf}$ protein activity at room temperature, and (2) depletion of the available $G\alpha_{olf}$ protein pool.

The α subunit of G protein has a molecular mass $\sim$40–50 kDa (Wilcox et al. 1994; Cao and Huang 2005), therefore its desorption is reliably detected by the SPR technique. However, quite low amplitude of signals measured can be ascribed to the low amount of receptors oriented in the direction allowing full access of $G\alpha_{olf}$ to GTP-γ-S. Indeed, the latter cannot penetrate the lipid bilayer to access $G\alpha_{olf}$ located inside the nanosome, whereas the hydrophobic

Fig. 4 Atomic force micros-
copy images with cross sectional
profiles corresponding to work-
ing "spots" of A1 (**a**) and A2 (**b**)
biofilms. Images were taken in
tapping mode after the second
day of using A1 and A2 biofilms
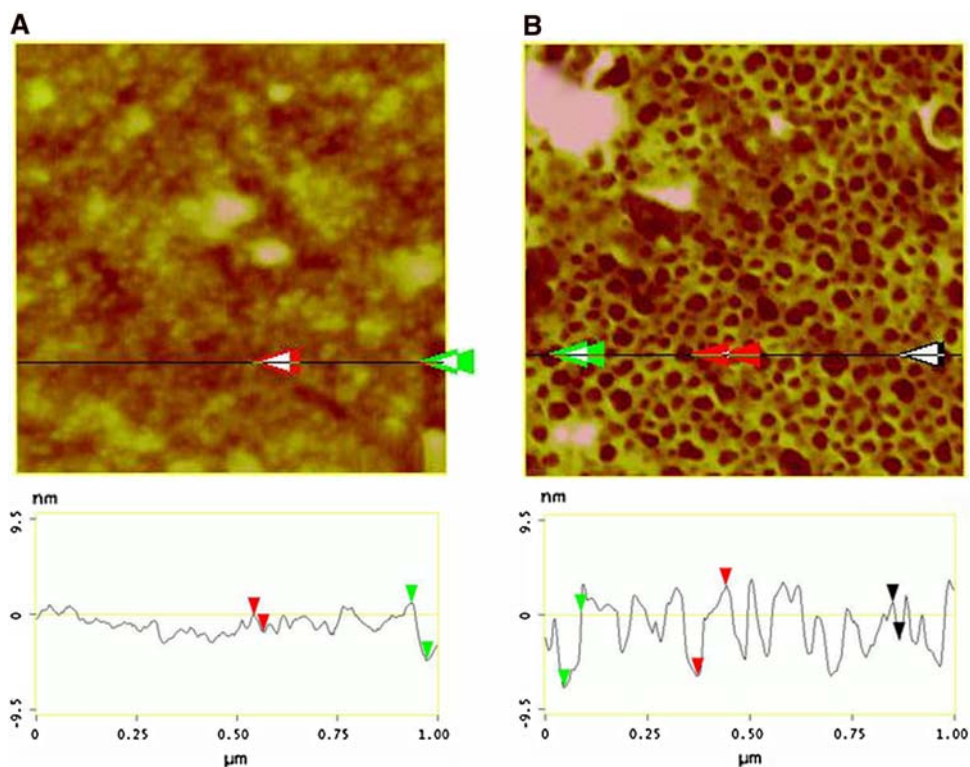for detection of odorants at room
temperature

Table 2 Biorecognition efficiency of various configurations (1, 2, 3)
of G protein-coupled olfactory receptor in a nanosome (see
Figs. 1b, 2b)

Configuration	1	2	3
Flexibility of N-end, crucial for odorant binding	−	+	+
Accessibility of $G\alpha_{olf}$ to GTP-γ-S	−	−	+
Biorecognition efficiency	Low	Middle	High

odorants may penetrate the bilayer (Ornskov et al. 2005;
Fujikawa et al. 2007) to reach the receptor ligand binding
pocket and activate the receptor.

Another phenomenon that could contribute to the optical
signal was the intrinsic conformational change of activated
OR. The latter is composed of a bundle of seven transmem-
brane α-helices connected by loops (Pearce et al. 2001).
Odorant stimulation of OR seems to induce a rearrange-
ment of helices 6 and 3 leading to separation of transmem-
brane domains in the helix bundle (Bourne 1997; Pearce
et al. 2001; Minic et al. 2005b). Recently it has been sug-
gested that the signal changes observed by SPR can be also
ascribed to the protein secondary structure changes. Thus,
May and Russell (May and Russell 2002) have correlated a
decrease in SPR signal to the formation of β-sheets, turn or
unordered protein secondary structures; compact helical
structure was thought to possess higher refractive index and
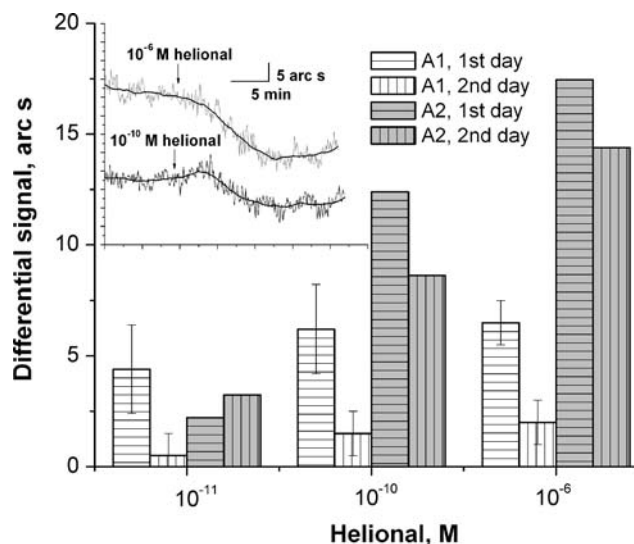thus to increase an SPR signal. In this way, the OR confor-

Fig. 5 Sensitivity of A1 and A2 biofilms to helional. The error values
mentioned represent intersensor standard deviation ($n = 2$–3). Inset:
typical kinetics of responses to helional obtained from the A2 biofilm
in differential mode; 50 point smoothing was applied to all curves

mational changes on SPR signals may also be taken into
consideration.

Two maxima bell-shaped curves such as that found pre-
viously (Vidic et al. 2006) can be superimposed to the
experimental points (Fig. 6) to account for the functional
response observed at the biofilm stimulation by the odorant
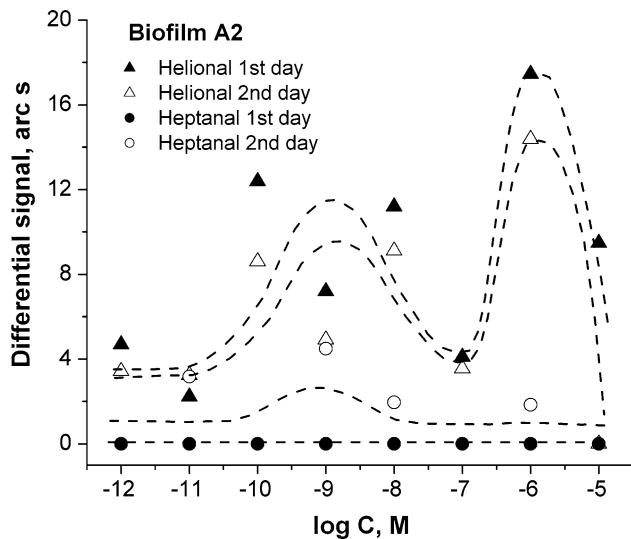specific for OR 17-40. Apart from the measurement at

Fig. 6 Profile of the A2 biofilm responses to helional during 2 days of work. Heptanal was used as a negative control. Data set was collected from the same sensor chip ($n = 1$)

10^{-9} M, which appears somewhat low for the measurements performed on both days for unclear reasons (which we assume may just be a case of the odorant dilution being made incorrectly), the general shape seems to be in good agreement with this profile. The hypothesis and model on the biological nature of such response profile are under testing.

Conclusion

It has been demonstrated that the density of nanosomes' adsorption and the multilayer bulk thickness are crucial points in design of the olfactory biofilms for the SPR-based screening of odorants. Sensitivity of the OR 17-40-bearing film to helional was specific and could be ascribed to two main molecular events actually undistinguishable from SPR signals: desorption of Gα protein from membrane bilayer and intrinsic conformational changes in activated OR itself. Further studies will clarify the mechanisms involved in odorant recognition by ORs at the biointerface.

References

Araneda RC, Kini AD, Firestein S (2000) The molecular receptive range of an odorant receptor. Nat Neurosci 3:1248–1255

Araneda RC, Peterlin Z, Zhang X, Chesler A, Firestein S (2004) A pharmacological profile of the aldehyde receptor repertoire in rat olfactory epithelium. J Physiol 555:743–756

Beketov GV, Shirshov YM, Shynkarenko OV, Chegel VI (1998) Surface plasmon resonance spectroscopy: prospects of superstrate refractive index variation for separate extraction of molecular layer parameters. Sens Actuators B Chem 48:432–438

Birnbaumer L (2007) Expansion of signal transduction by G proteins. The second 15 years or so: from 3 to 16 α subunits plus $\beta\gamma$ dimers. Biochim Biophys Acta 1768:756–771

Bourne HR (1997) How receptors talk to trimeric G proteins. Curr Opin Cell Biol 9:134–142

Cao Y, Huang Y (2005) Palmitoylation regulates GDP/GTP exchange of G protein by affecting the GTP-binding activity of Goα. Int J Biochem Cell Biol 37:637–644

Crowe ML, Perry BN, Connerton IF (2000) G$_{olf}$ complements a GPA1 null mutation in *Saccharomyces cerevisiae* and functionally couples to the STE2 pheromone receptor. J Recept Signal Transduct Res 20:61–73

Dannenberger O, Weiss K, Himmel H-J, Jager B, Buck M, Woll C (1997) An orientation analysis of differently endgroup-functionalised alkanethiols adsorbed on Au substrates. Thin Solid Films 307:183–191

Fujikawa M, Nakao K, Shimizu R, Akamatsu M (2007) QSAR study on permeability of hydrophobic compounds with artificial membranes. Bioorg Med Chem 15:3756–3767

Hou Y, Jaffrezic-Renault N, Martelet C, Zhang A, Minic-Vidic J, Gorojankina T, Persuy MA, Pajot-Augy E, Salesse R, Akimov V, Reggiani L, Pennetta C, Alfinito E, Ruiz O, Gomila G, Samitier J, Errachid A (2007) A novel detection strategy for odorant molecules based on controlled bioengineering of rat olfactory receptor I7. Biosens Bioelectron 22:1550–1555

Johnsen S, Widder EA (1999) The physical basis of transparency in biological tissue: ultrastructure and the minimization of light scattering. J Theor Biol 199:181–198

Jones DT, Reed RR (1989) Golf: an olfactory neuron specific G-protein involved in odorant signal transduction. Science 244:790–795

Ko HJ, Park TH (2005) Piezoelectric olfactory biosensor: ligand specificity and dose-dependence of an olfactory receptor expressed in a heterologous cell system. Biosens Bioelectron 20:1327–1332

Ko HJ, Park TH (2006) Dual signal transduction mediated by a single type of olfactory receptor expressed in a heterologous system. Biol Chem 387:59–68

Levasseur G, Persuy MA, Grebert D, Remy JJ, Salesse R, Pajot-Augy E (2003) Ligand-specific dose-response of heterologously expressed olfactory receptors. Eur J Biochem 270:2905–2912

Li G, Ferrie AM, Fang Y (2006) Label-free profiling of ligands for endogenous GPCRs using a cell-based high-throughput screening technology. JALA 11:181–187

Liu Q, Cai H, Xua Y, Li Y, Li R, Wang P (2006) Olfactory cell-based biosensor: a first step towards a neurochip of bioelectronic nose. Biosens Bioelectron 22:318–322

Marrakchi M, Vidic J, Jaffrezic-Renault N, Martelet C, Pajot-Augy E (2007) A new concept of olfactory biosensor based on interdigitated microelectrodes and immobilized yeasts expressing the human receptor OR17-40. Eur Biophys J 36:1015–1018. doi:10.1007/s00249-007-0187-6

May LM, Russell DA (2002) The characterization of biomolecular secondary structures by surface plasmon resonance. Analyst 127:1589–1595

Milligan G (2006) G-protein-coupled receptor heterodimers: pharmacology, function and relevance to drug discovery. Drug Discov Today 11:541–549

Minic J, Persuy MA, Godel E, Aioun J, Connerton I, Salesse R, Pajot-Augy E (2005a) Functional expression of olfactory receptors in yeast and development of a bioassay for odorant screening. FEBS J 272:524–537

Minic J, Sautel M, Salesse R, Pajot-Augy E (2005b) Yeast system as a screening tool for pharmacological assessment of G protein coupled receptors. Curr Med Chem 12:763–771

Monk BC, Montesinos C, Leonard K, Serrano R (1989) Sidedness of yeast plasma membrane vesicles and mechanisms of activation of the ATPase by detergents. Biochim Biophys Acta 981:226–234

Ornskov E, Gottfries J, Erickson M, Folestad S (2005) Experimental modelling of drug membrane permeability by capillary electrophoresis using liposomes, micelles and microemulsions. J Pharm Pharmacol 57:435–442

Pearce TC, Verschure PF, White J, Kauer JS (2001) Stimulus encoding during the early stages of olfactory processing: a modeling study using an artificial olfactory system. Neurocomputing 38–40:299–306

Seckler R, Wright JK (1984) Sidedness of native membrane vesicles of *Escherichia coli* and orientation of the reconstituted lactose: H$^+$ carrier. Eur J Biochem 142:269–279

Sung JH, Ko HJ, Park TH (2006) Piezoelectric biosensor using olfactory receptor protein expressed in *Escherichia coli*. Biosens Bioelectron 21:1981–1986

Tollin G, Salamon Z, Hruby VJ (2003) Techniques: plasmon-waveguide resonance (PWR) spectroscopy as a tool to study ligand–GPCR interactions. Trends Pharmacol Sci 24:655–659

Vidic JM, Grosclaude J, Persuy MA, Aioun J, Salesse R, Pajot-Augy E (2006) Quantitative assessment of olfactory receptors activity in immobilized nanosomes: a novel concept for bioelectronic nose. Lab Chip 6:1026–1032

Vidic J, Pla-Roca M, Grosclaude J, Persuy MA, Monnerie R, Caballero D, Errachid A, Hou Y, Jaffrezic-Renault N, Salesse R, Pajot-Augy E, Samitier J (2007) Gold surface functionalization and patterning for specific immobilization of olfactory receptors carried by nanosomes. Anal Chem 79:3280–3290

Wetzel CH, Oles M, Wellerdieck C, Kuczkowiak M, Gisselmann G, Hatt H (1999) Specificity and sensitivity of a human olfactory receptor functionally expressed in human embryonic kidney 293 cells and *Xenopus laevis* oocytes. J Neurosci 19:7426–7433

Wilcox MD, Schey KL, Dingus J, Mehta ND, Tatum BS, Halushka M, Finch JW, Hildebrandt JD (1994) Analysis of G protein γ subunit heterogeneity using mass spectrometry. J Biol Chem 269:12508–12513